Am J Transl Res 2024;16(9):4343-4354
www.ajtr.org /ISSN:1943-8141/AJTR0157347

Original Article

Morphine sulfate nano-controlled release microspheres effectively relieve visceral pain caused by tumor in mice

Yan Zhou, Lei Feng

Department of Pain, Beijing Jishuitan Hospital, Capital Medical University, Beijing 100035, China

Received April 22, 2024; Accepted June 20, 2024; Epub September 15, 2024; Published September 30, 2024

Abstract: Objective: This work aimed to demonstrate the effect of morphine sulfate nano-controlled release microspheres in relieving tumor-induced visceral pain. Methods: The morphine sulfate nano-controlled release microspheres were prepared and optimized, and their drug release properties *in vitro* were explored. Chitosan sustained-release microspheres were used to prepare morphine sulfate nanospheres for controlled release. Forty C57BL/6J mice were utilized, divided into a control group (Control, n=10) and a model group (Model, n=30). An intrapancreatic cancer pain model was established using mPA^{KPC}-luc cells. Mice in the model group were further categorized into the following groups: a blank control group (injected with blank chitosan sustained-release microspheres, Blank, n=10), a Nano + morphine group (injected with morphine-chitosan sustained-release microspheres, Nano + morphine, n=10), and a morphine sulfate group (injected with morphine sulfate, Morphine, n=10). Behavioral assessments were conducted to evaluate pain sensitivity by examining monoamine neurotransmitter levels in the thalamus. Abdominal mechanical allodynia tests and premonition scoring were employed to assess pain perception. Adverse reactions were monitored to evaluate the efficacy and safety profile of morphine sulfate nanospheres. Results: The cumulative drug release rate *in vitro* was as high as 99.8% when the amount of crosslinking agent was 8:1. In the Model group, mice exhibited a significant increase in writhing responses due to tumor-induced pain ($P < 0.05$). Compared to the Blank group, both the Nano + morphine and Morphine groups showed a significant reduction in writhing responses and premonition scores following drug administration ($P < 0.05$). Additionally, the pain threshold increased ($P < 0.05$), accompanied by elevation in hypothalamic serotonin (5-HT) levels ($P < 0.05$) and a decrease in norepinephrine (NE) level ($P < 0.05$). Furthermore, no significant adverse reactions were observed in these groups. Conclusions: Morphine sulfate nano-controlled release microspheres exhibit favorable drug release kinetics, demonstrating notable therapeutic efficacy in reliving tumor-induced visceral pain and extending the duration of pain relief. Furthermore, they demonstrate a good safety profile without inducing adverse effects, underscoring their significant clinical value. The results support continued clinical application and promotion of morphine sulfate nano-controlled release microspheres.

Keywords: Morphine sulfate nano-controlled release microspheres, visceral pain, tumor, pain score

Introduction

A patient's quality of life (QoL) may be significantly compromised by both the physical pain and psychological distress induced by tumor and its treatment regimen. Pain can be categorized temporally as acute or chronic, and mechanistically as physical nociceptive, visceral nociceptive, idiopathic, total pain, among others [1, 2]. Visceral pain arises from injury to internal organs and stimulation of pain receptors within them, manifesting as sensations perceived along afferent nerves originating from the affected organs. Tumor-induced visceral pain presents as deep, inaccurately localized discomfort, characterized by dull, pulling, or colicky sensations. Most patients perceive the painful area to be larger than the visceral area of the diseased part, which exacerbates their suffering [3]. Opioids remain the oldest, most efficacious, safest, and preferred analgesic class to date. They exert potent analgesic effects with a relatively low incidence of long-term medication side effects. Particularly for patients experiencing moderate to severe pain, opioids represent indispensable therapeutic agents [4, 5]. Among opioids, morphine stands as the quintessential representative

https://doi.org/10.62347/XVOZ6080

Table 1. Composition of morphine sulfate nano-controlled release microspheres

Composition	Amount
Chitosan	100 mg
Morphine acetate monosulfate injection	2%
Soybean oil for injection	15 mL
Span80	15 mL
Sodium Tripolyphosphate	Span80

and remains the most widely used medication in clinical settings. Moreover, recent years have witnessed the clinical use of novel opioid formulations with high therapeutic efficacy and minimal adverse effects [6, 7]. Consequently, the development of novel sustained-release analgesic formulations is of paramount importance.

Nano-controlled release microspheres offer precise drug release modulation, heightened drug targeting, enhanced permeability of hydrophobic drug molecules across cell membranes, improved drug stability, and altered routes of administration. Encapsulation of drugs within chitosan microspheres extends their therapeutic efficacy. Naoi et al. [6] utilized palmitoyl ascorbate as a cross-linking agent to fabricate insulin microspheres, achieving sustained insulin release for up to 80 hours. Koklesova et al. [7] investigated the *in vivo* release of progesterone and chitosan microspheres, and the plasma concentration of the microspheres was maintained at 12 ng/mL within 5 months of intramuscular injection of the microspheres into rabbits. Immediate-release opioid analgesics typically necessitate administration every 3-4 hours, resulting in rapid fluctuations in blood concentration. This dynamic can lead to terminal dose failure in some patients, characterized by escalated pain and inappropriate medication management [8]. Nano-controlled release microspheres offer a solution by regulating the release rate of analgesics, thereby sustaining blood concentration within the therapeutic range and minimizing fluctuation [9]. While simple morphine sustained-release tablets can provide sustained analgesic effects, they present limitations such as unstable drug release rate, large fluctuations in blood drug concentration, and inconsistent treatment effects caused by individual differences among patients. Long-term use of morphine can also lead to side effects and dependence. However, the stability of nanoparticles suggests that morphine sulfate nano-controlled release microspheres may effectively overcome these shortcomings. Nano-controlled release technology can achieve slow and sustained drug release *in vivo*, maintaining stable blood drug concentration, reducing administration frequency, and reducing the peak to valley concentration difference of drugs in vivo, thereby reducing side effects [10, 11]. In addition, nano-level drug carriers can also improve drug targeting, reduce the impact on non-target tissues, and improve treatment efficacy. Avantil, a morphine sulfate sustained-release capsule from Kings Pharmaceuticals of the United States, uses a combination of immediate-release and sustained-release pellets. After oral administration, 10% of the sustained-release pellets quickly release morphine, and the rest is slowly released within 24 hours, solving the problem of rapid and long-term pain relief [12]. Therefore, the preparation of morphine sulfate nano-controlled release microspheres is of great significance for improving the therapeutic effect of visceral pain caused by tumors.

This study applied nano-controlled release technology to the preparation of anesthesia drug morphine, optimized the preparation process of morphine sulfate nano-controlled release microspheres, and explored their *in vitro* drug release performance. The therapeutic effects of morphine sulfate nano-controlled release microspheres on tumor-induced visceral pain were investigated. The results may provide a reference for the future clinical treatment of alleviating visceral pain caused by tumors.

Materials and methods

Preparation of morphine sulfate nano-controlled release microspheres

The components of morphine sulfate nano-controlled release microspheres are shown in **Table 1**. Preparation method was as follows: 100 mg of chitosan (Sangon Biotechnology (Shanghai) Co., Ltd., China) (degree of deacetylation ≥ 90% and molecular weight was 50,000) was dissolved with 2% morphine acetate monosulfate injection (Qinghai Pharmaceutical Factory Co., Ltd., China) to prepare a chitosan solution with a concentration of 20 mg/

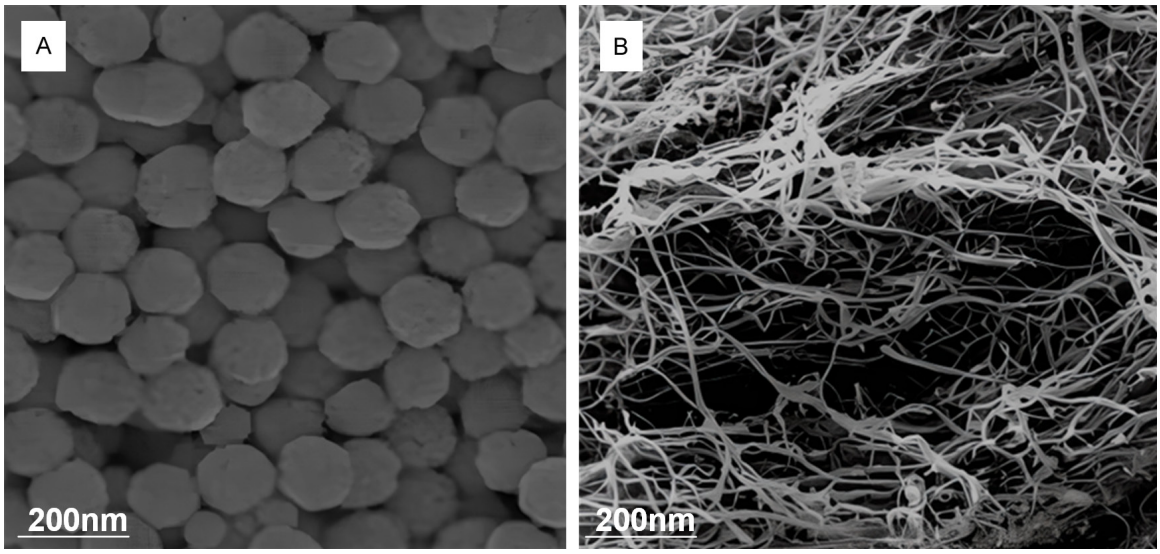

Figure 1. Scanning electron microscopy images. A: Morphine sulfate nano-controlled release microspheres; B: Single-walled carbon nanotubes.

mL. Then, 15 mL of soybean oil for injection (Tieling Beiya Medicinal Oil Co., Ltd., China) was mixed with 0.75 mL of Span80 for water bath at 36°C, which was stirred for 10 minutes. Afterwards, the chitosan solution was added into the oil to emulsify for 1.5 hours, which was stirred at a speed of 700 rpm. Finally, 10 mg/mL sodium tripolyphosphate (Sangon Biotechnology (Shanghai) Co., Ltd., China) was slowly dropped into a microinjection pump (Longer Constant Flow Pump Co., Ltd., UK) for cross-linking for 2 hours, and centrifuged at 1,000 rpm for 1 minute to remove oil. The resulting microspheres were washed with acetone (Sangon Biotechnology (Shanghai) Co., Ltd., China) for 2 times, which was subjected to dehydration with absolute ethanol (Sangon Biotechnology (Shanghai) Co., Ltd., China), ultrasonic dispersion, and vacuum drying [13]. After preparation, high-speed scanning electron microscope HEM6000 (Guoyi Quantum Technology (Hefei) Co., Ltd.) was employed for observation. The image is shown as **Figure 1A**.

In vitro drug release performance of morphine sulfate nano-controlled release microspheres

First, a standard curve of morphine sulfate was established, and the specific operation was as follows. 1 mL of morphine sulfate injection (a concentration of 10 mg/mL) was taken out, which was diluted to 50 mL using 0.2 mol/mL phosphate buffer (pH=7.4) to prepare stock solution. Next, 5 mL of the stock solution was absorbed and diluted to prepare standard solutions with concentrations of 10 g/mL, 50 g/mL, 100 g/mL, 150 g/mL, 200 g/mL, and 500 g/mL, respectively. Finally, ultraviolet (UV)-visible (Vis) spectrophotometer (Shanghai Yidian Analytical Instrument Co., Ltd., China) was employed to measure the absorbance at the wavelength of 250 nm, to construct the standard curve regression equation.

Secondly, microspheres were prepared by the previous method, and their single-walled carbon nanotubes were observed by electron microscope (Carl Zeiss Optics (China) Co., Ltd., Germany) and photographed (**Figure 1B**). Morphine sulfate was added at 40% of the chitosan mass, and the cross-linking agent was cross-linked at the rate of 1.4 mL/h at 1/4, 1/6, and 1/8 of the chitosan mass for 2 hours, respectively. The drug loading, encapsulation rate, and drug release property *in vitro* were determined, respectively.

The determination of drug loading and encapsulation efficiency were as follows: 25 mg of morphine sulfate nano-controlled release microspheres were fully swollen in 25 mL of phosphate buffer, followed by ultrasonic crushing, mixing, and filtration. Subsequently, the filtrate was collected for absorbance determination. The concentration of morphine sulfate was calculated using the regression equation

of the standard curve. The equations (1) and (2) were employed to express the drug loading, and encapsulation efficiency of morphine sulfate nano-controlled release microspheres, respectively.

$$\text{Drug loading} = \frac{A}{B} \times 100\% \quad (1)$$

$$\text{Packing rate} = \frac{C}{D} \times 100\% \quad (2)$$

In the above equations, *A* stands for the amount of drug contained in the microspheres, *B* represents the total amount of the microspheres, *C* means the amount of drug encapsulated in the microspheres, and *D* indicates the total amount of drug injected.

The *in vitro* drug release performance of morphine sulfate nano-controlled release microspheres was determined, and the specific operation was as follows. On a constant temperature shaker (37°C and 100 r/min), 25 mg of the prepared morphine sulfate nano-controlled release microspheres were placed in a dialysis bag with 25 mL of phosphoric acid. Phosphate buffer (0.2 mol/mL and pH=7.4) was used as the medium, and 2 mL of it was sampled at the 1st hour, the 4th hour, the 8th hour, the 24th hour, the 48th hour, and the 72nd hour respectively. After adding the medium under the same conditions, the absorbance at 250 nm was measured and the cumulative release rate was calculated according to the standard curve.

Materials

Forty healthy C57BL/6J mice (specific pathogen-free, SPF grade) (Saiye Biotechnology Co., Ltd., China), aged 6-8 weeks with an average weight of (200.52 ± 18.14) g, were purchased from Jiangsu Cavens Experimental Animals Co., Ltd. (China). They were housed in the animal facility of our institution under standard conditions with a temperature of 24°C and a 12-hour light-dark cycle. The mice had free access to food and water and were acclimatized for one week prior to the experiments. The research flow chart is detailed in **Figure 2**.

Establishment of pancreatic cancer-induced visceral pain model

mPA^{KPC}-luc cells were obtained from Jiangsu Jicui Yaokang Biotechnology Co., Ltd. (China) to establish a murine model of pancreatic cancer-induced visceral pain. The method involved resuscitating mPA^{KPC}-luc cells and performing serial passaging using 90% Dulbecco's modified Eagle's medium (DMEM) + 10% fetal calf serum (FBS) culture medium for maintenance (Thermo Fisher Scientific Inc., USA). Log-phase growth mPA^{KPC}-luc cells were harvested, washed with phosphate-buffered saline (PBS), and then suspended in fresh culture medium. Cell viability was assessed prior to implantation. A 100 μL mixture of mPA^{KPC}-luc cells and matrix gel (1:1 ratio with PBS) was prepared under sterile conditions and injected into mice. Tumor growth was monitored for seven days, and tumor burden was measured using an *in vivo* imaging system. Mice with comparable tumor sizes were selected to minimize variability in subsequent behavioral assessment. At twelve days post mPA^{KPC}-luc cell injection, visceral pain was assessed using abdominal mechanical allodynia tests and premonition scoring. The development of acute visceral pain was confirmed by observing behaviors such as repeated squatting and licking of the abdomen or lower belly, head twisting towards the back while licking the tail or hindquarters, shoulder shrugging with hind legs standing upright and abdomen contracting, hind legs stretched backward with abdomen flat on the ground, elongation of the body with muscle tremors, noticeable abdominal contractions, or body twisting. The appearance of these symptoms indicated successful establishment of the acute visceral pain model.

Experimental grouping

Ten mice received intraperitoneal injection of 100 μL of mixed culture medium as the control group (Control), while the remaining 30 mice were designated as the model group (Model). Within the Model group, mice were further divided into the following subgroups: blank chitosan sustained-release microsphere control group (Blank, n=10), nano-morphine chitosan sustained-release microsphere group (Nano + morphine, n=10), and morphine sulfate group (Morphine, n=10). One hour after successful model establishment, mice had their dorsal fur shaved and skin prepared. Subsequently, each group received injections of equal volumes of saline, blank chitosan sustained-release microspheres, morphine sulfate (3 mg/kg), or mor-

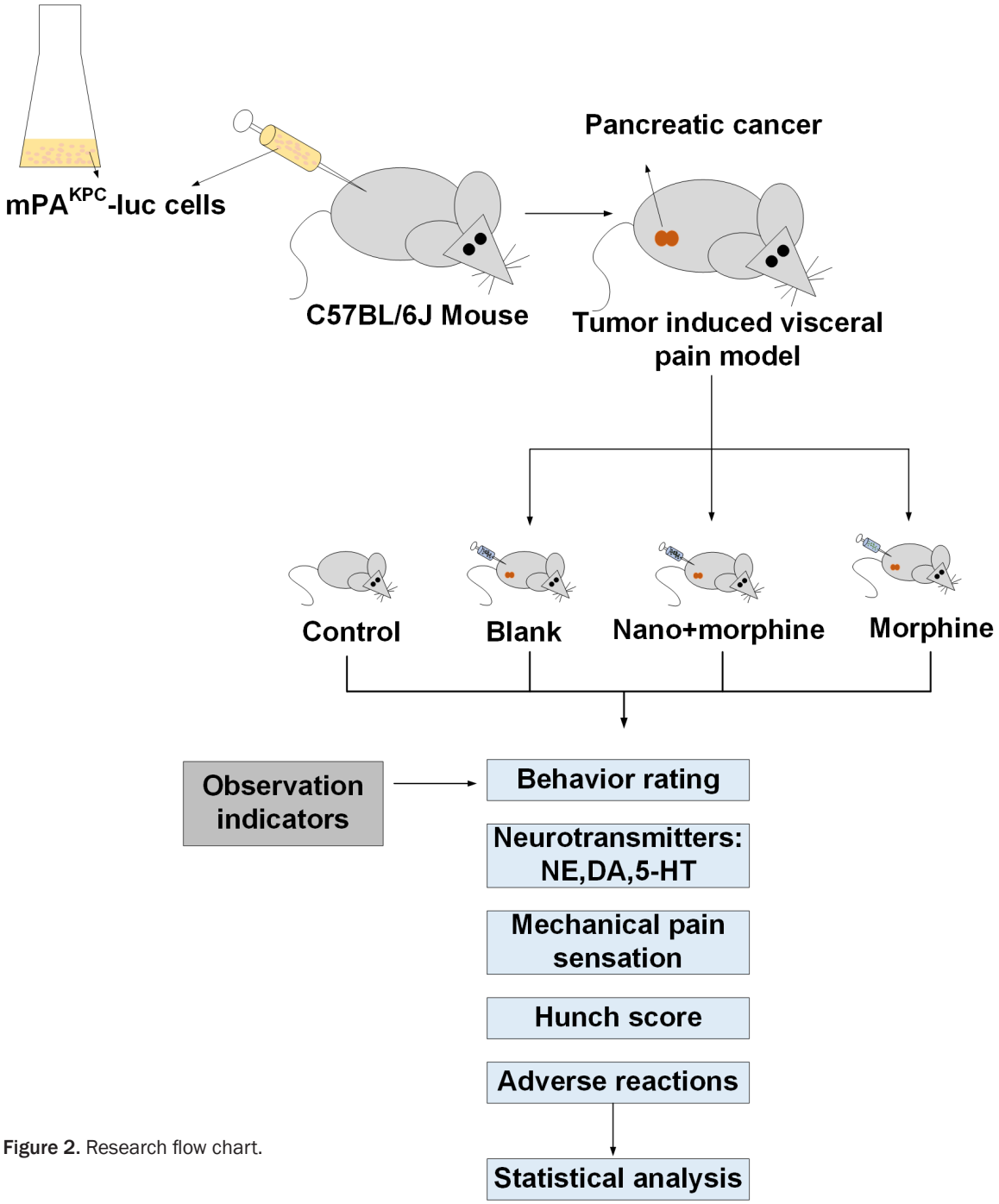

Figure 2. Research flow chart.

phine sulfate chitosan sustained-release microspheres (15 mg/kg).

Outcome measures

(1) Behavioral scoring. Following drug administration, mouse behavior was observed and scored according to the Schmauss scoring criteria: normal posture was scored as 0, backward body twisting as 1, hind legs stretched backward with abdomen flat on the ground as 2, and abdominal muscle contraction as 3. The drug inhibition rate was calculated based on the frequency of writhing behavior exhibited by the mice.

$$IR(\%) = \frac{Control_{ANOBT} - Medicine_{ANOBT}}{Control_{ANOBT}} \quad (3)$$

IR: inhibition rate; ANOBT: average number of body twists.

(2) Measurement of monoamine neurotransmitters in the brain. One hour after drug treatment, the mice were euthanized using cervical dislocation and immediately placed in an icebox. The whole brain tissue was removed from the mice in the icebox, and the thalamus was separated and weighed. The thalamus tissue was then homogenized to obtain a uniform paste, which was subsequently centrifuged (15,000 rpm for 15 minutes) to collect the supernatant. High-performance liquid chromatography (HPLC) using a Waters RP18 column was employed to analyze the supernatant and observe peak values. The mobile phase consisted of a solution containing 2.5 g of sodium octanesulfonate ($C_8H_{19}NaO_4S$), 13.6 g of potassium dihydrogen phosphate (KH_2PO_4), and 36.2 g of ethylenediaminetetraacetic acid (EDTA) in 1,000 mL of water, adjusted to a pH of 3.4 using phosphate buffer. The mobile phase composition was acetonitrile: methanol: water =3:19:78. The analysis was conducted at room temperature with the following parameters: Range: 200 nA; Ee: +0.7 V; Filt: 0.1 Hz. Monoamine neurotransmitters analyzed included norepinephrine (NE), serotonin (5-HT), and dopamine (DA).

(3) Abdominal mechanical allodynia test. Prior to model establishment, before drug administration, and at 10 min, 30 min, 1 h, 2 h, 4 h, 6 h, 9 h, and 12 h post-drug administration, Von Frey filaments were vertically applied to the left upper abdomen of mice for approximately 2 s to determine the pain threshold (defined by mouse writhing or vocalization response).

(4) Premonition scores. Premonitory behaviors were assessed to evaluate visceral pain in mice. The scoring method included: mice displaying exploratory behavior and normal coat gloss scored 0; mice with a rounded back and exploratory behavior scored 1; mice with a rounded back, reduced exploratory behavior, disheveled fur, and intermittent abdominal contractions scored 2; mice with a severely rounded back, significantly reduced exploratory behavior, and intermittent abdominal contractions scored 3; mice with a severely rounded back, minimal exploratory behavior, and huddled head scored 4. Mice were individually placed on a platform and observed for 5 minutes, and the average score was recorded as the premonition score.

(5) Adverse reactions. Following drug administration, observations were made for changes in mouse respiration, corneal reflex, and stiffness, to determine the incidence of adverse reactions.

Statistical analysis

SPSS23.0 was used for data analyses. Measured data were denoted as mean ± standard deviation ($\bar{x} \pm s$), which was tested by *t* test, repeated measures analysis of variance (ANOVA), or one way ANOVA followed by Turkey test, as appropriate. Counted data were tested by χ^2 test for comparison of intergroup rate (%). $P < 0.05$ indicated a significant difference.

Results

Effect of different crosslinker dosages on drug loading capacity and encapsulation efficiency of morphine sulfate nano-controlled release microspheres

Figure 3A shows linear regression of the absorbance with morphine hydrochloride concentration. The regression equation is y=0.006x + 0.0137, and the coefficient of determination R^2=0.9998, indicating that the correlation between absorbance and concentration was good within this range.

Figure 3B indicates the effect of different crosslinking agent dosages on the drug loading and encapsulation efficiency of morphine sulfate nano-controlled release microspheres. When the crosslinking agent dosage was 4:1, 6:1, and 8:1, the drug loading was 10.2%, 12.5%, and 15.1% in turn and encapsulation rates were 43.2%, 48.2%, and 57.0%, respectively. Variance analysis of multiple samples reveals that the impacts of different crosslinking agent dosages on drug loading and encapsulation rate were substantial ($P < 0.05$).

Drug release profiles of morphine sulfate nano-controlled release microspheres at different crosslinker dosages

Figure 4 displays the drug release curve of morphine sulfate nano-controlled release microspheres under different crosslinking agent dosages. The cumulative release rates

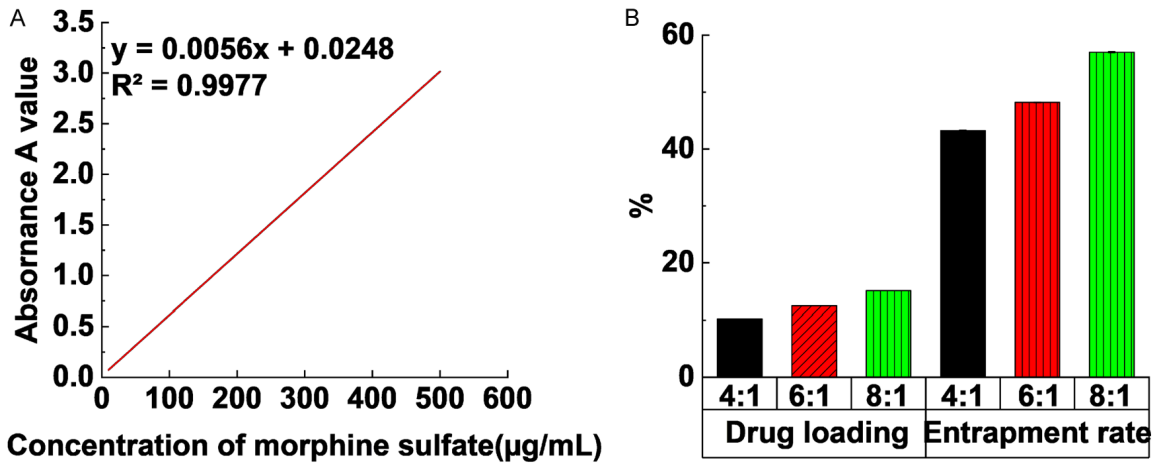

Figure 3. *In vitro* drug release performance of morphine sulfate nano-controlled release microspheres. A: Standard curve of morphine sulfate; B: The effect of different crosslinking agent dosages on drug loading and encapsulation efficiency of morphine sulfate nano-controlled release microspheres.

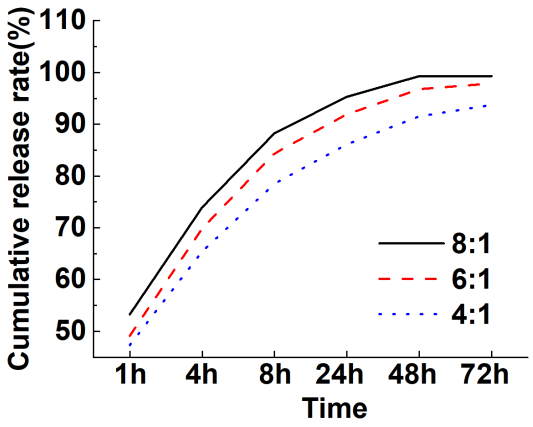

Figure 4. Drug release curves of morphine sulfate nano-controlled release microspheres with different cross-linking agent dosages.

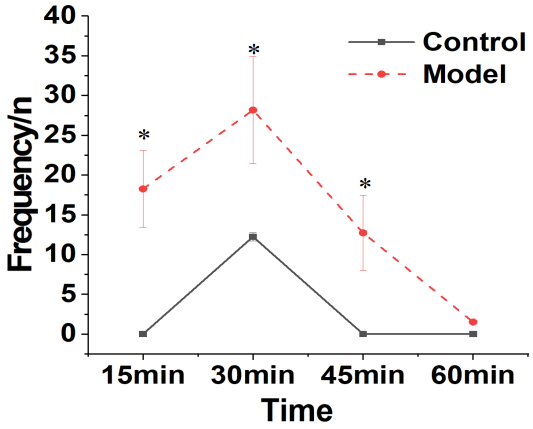

Figure 5. Comparison of behavioral responses between Control and Model groups of mice. Note: *compared to the Control group, $P < 0.05$.

were 64.6%, 69.9%, and 74.6%, respectively when the cross-linking agent dosage was 4:1, 6:1, and 8:1 within 4 hours of drug release. After 72 hours, the drug release was relatively complete, reaching 94.6%, 98.6%, and 99.8%, respectively. In addition, the cumulative drug release rate of the cross-linking agent dosage of 8:1 was always higher than the rate of cross-linking agent dosage of 6:1 and 4:1 in the whole process, suggesting that the release rate of cross-linking agent of 8:1 was the highest.

Comparison of behavioral responses between Control and Model groups of mice

Behavioral changes were seen in mice from the Control and Model groups following injection of mPA^{KPC}-luc cells. The findings are illustrated in **Figure 5**. Mice in the Model group demonstrated a significant increase in body twisting behaviors 12 days post-intraperitoneal modeling, in comparison to the Control group ($P < 0.05$). Mice in the normal group occasionally exhibited movement.

Inhibitory effect of morphine sulfate nano-controlled release particles on visceral pain response in mice with pancreatic cancer

As shown in **Figure 6**, compared to the Blank group, mice in the Nano + morphine and Morphine groups exhibited a significant reduction in the number of pain-induced body twists following treatment ($P < 0.05$). Morphine sulfate nano-controlled release particles demon-

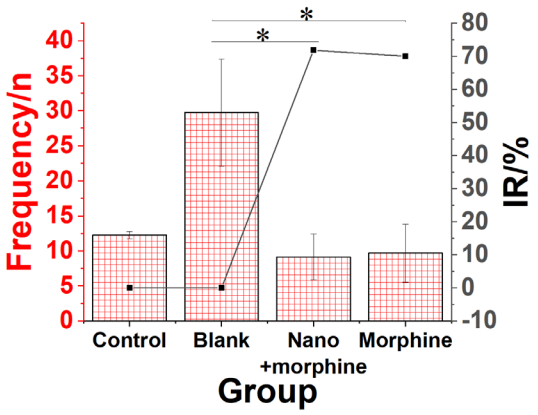

Figure 6. Inhibitory effect of morphine sulfate nano-controlled release particles on visceral pain response in mice with pancreatic cancer. Note: *compared to the Blank group, $P < 0.05$.

strated a pronounced inhibitory effect on visceral pain response in mice with pancreatic cancer, and the pain inhibition rate in the Nano + morphine group was slightly higher compared to the Morphine group.

Effect of morphine sulfate nano-controlled release particles on brain neurotransmitters in mice with pancreatic cancer-induced visceral pain model

Compared to the Blank group, morphine sulfate nano-controlled release particles significantly decreased the levels of NE while significantly increasing the 5-HT levels in the brains of mice in the pancreatic cancer-induced visceral pain model (all $P < 0.05$). There were no significant changes in DA levels in the brains of mice from the Control, Blank, Nano + morphine, and Morphine groups ($P > 0.05$). **Figure 7** shows the detailed results.

Changes in pain thresholds of mice before and after administration

As shown in **Figure 8**, mice in the Blank group exhibited significantly lower pain thresholds compared to mice in the Control group ($P < 0.05$). Furthermore, compared to the Blank group, mice in the Nano + morphine and Morphine groups demonstrated a significant increase in pain thresholds following treatment (all $P < 0.05$). Moreover, mice in the Nano + morphine group exhibited longer-lasting pain relief compared to the Morphine group.

Effect of morphine sulfate nano-controlled release particles on premonition score of mice with pancreatic cancer-induced visceral pain

As shown in **Figure 9**, compared to the Blank group, mice in the Nano + morphine and Morphine groups exhibited a significant reduction in premonition scores following treatment (all $P < 0.05$).

Physiologic toxicity responses of mice after administration

As depicted in **Figure 10**, mice in the Control, Blank, and Nano + morphine groups did not exhibit significant adverse reactions. However, in the Morphine group, there was a 24% incidence of respiratory depression, an 18% incidence of corneal reflex disappearance, and a 36% incidence of rigidity.

Discussion

The visceral pain caused by tumors has a large dispersion range and is often accompanied by autonomic nervous reactions such as traction pain, sweating, skin vasoconstriction, and intestinal peristalsis enhancement. This pain is severe and persistent [14]. It is estimated by the World Health Organization (WHO) that four million patients suffer from the pain, and most patients do not get effective control, particularly in developing countries. Moreover, pain relief is considered a fundamental human right. In the context of cancer patients, unmitigated pain is deemed unacceptable, given that effective pain management is achievable. Therefore, medical professionals bear the responsibility of alleviating pain for patients [15-17].

In clinical settings, medical practitioners employ both painful treatment interventions and analgesics to enhance the quality of life and overall health of patients. In the current study, morphine sulfate nano-controlled release microspheres were formulated and optimized to explore their *in vitro* drug release characteristics. The results showed that when the crosslinking agent dosage was 8:1, the drug loading and encapsulation rate were 15.1% and 57.0%, respectively, which were higher than that when the crosslinking agent dosage was 6:1 and 4:1. Within 4 hours of drug release, the cumulative release rate was 74.6%. After 72 hours, the drug release rate was

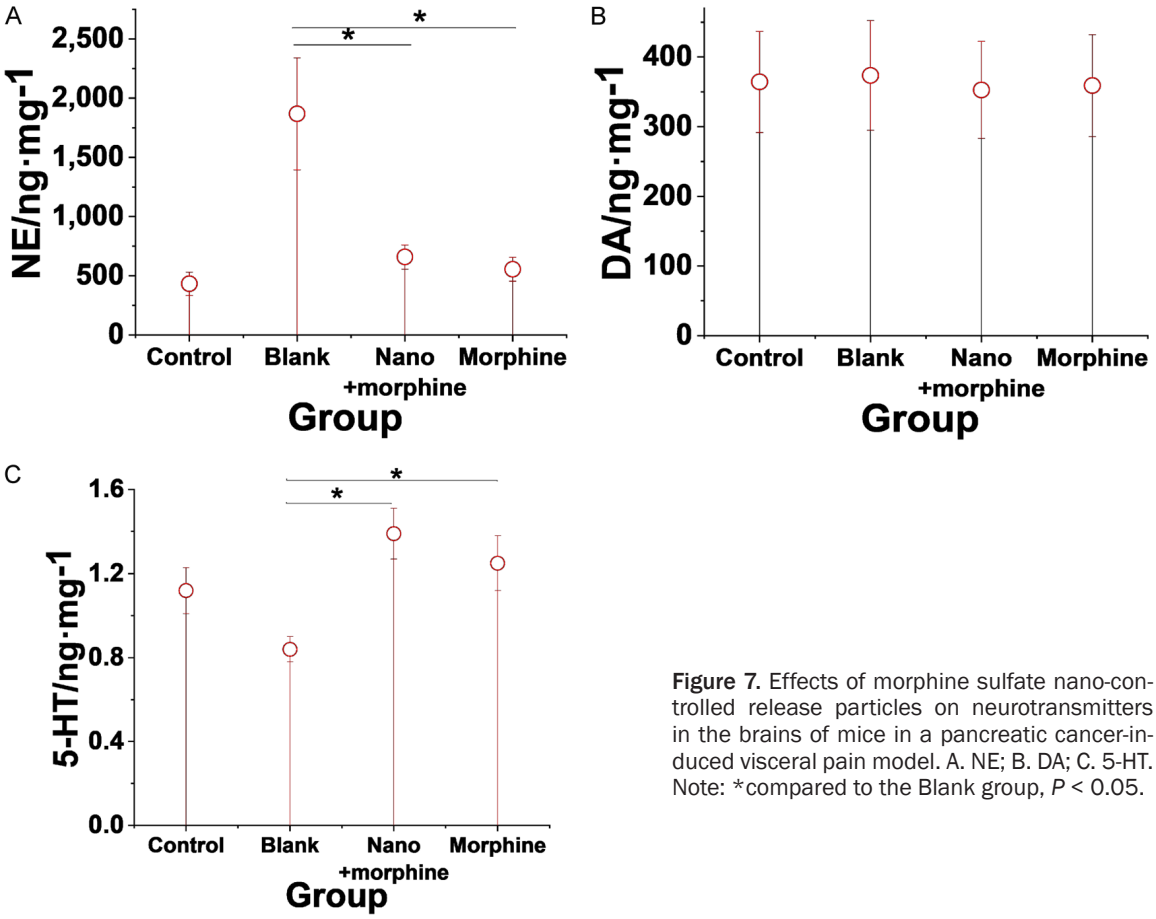

Figure 7. Effects of morphine sulfate nano-controlled release particles on neurotransmitters in the brains of mice in a pancreatic cancer-induced visceral pain model. A. NE; B. DA; C. 5-HT. Note: *compared to the Blank group, $P < 0.05$.

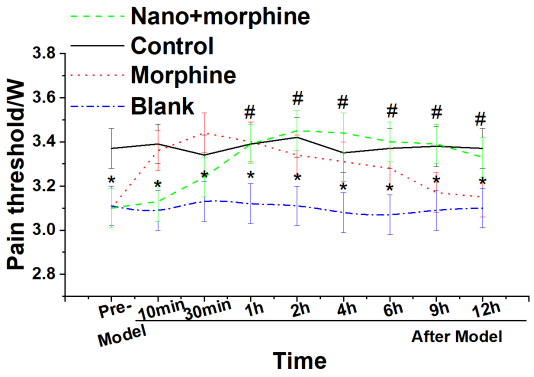

Figure 8. Changes in pain threshold before and after administration in each group of mice. Note: *compared to the Blank group, $P < 0.05$; #compared to the Control group, $P < 0.05$.

99.8%. This indicates that the preparation method in this study can improve the *in vitro* drug release performance of morphine sulfate nano-controlled release microspheres. It has a good release rate and pharmacokinetic characteristics.

This study employed a KPC cell-induced pancreatic cancer model to investigate the *in vivo* efficacy and safety of morphine sulfate nano-controlled release particles. Wang et al. found that implanting KPC cells into healthy mice can establish a tumor-associated visceral pain model [18]. In our study, after twelve days of modeling, mice exhibited reduced exploratory behavior, disheveled fur, and noticeable abdominal contractions, which aligns with their findings. Moreover, the decreased abdominal pain threshold and increased premonition scores indicate the successful establishment of a cancer-induced visceral pain model in this study. Pain perception is associated with stimuli received by the hypothalamus, where monoamine neurotransmitters such as 5-HT and NE are involved in regulating pain sensation. Specifically, 5-HT acts through 5-HT2 receptors, and NE acts thorugh adrenergic receptors to impede the transmission of nociceptive impulses, thereby reducing pain sensitivity. In a study of Nemoto et al., agonists and antago-

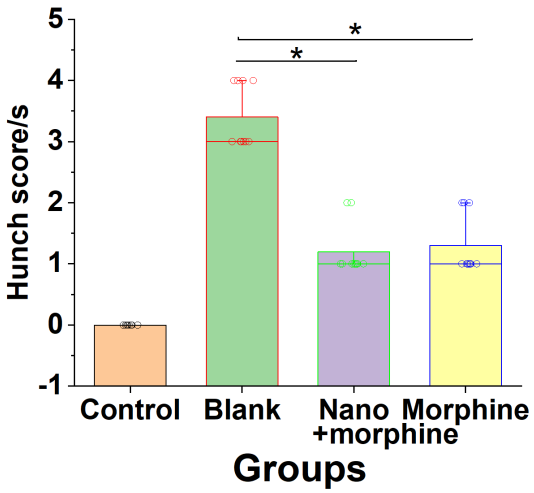

Figure 9. Effect of morphine sulfate nano-controlled release particles on premonitory pain scores in mice with pancreatic cancer-induced visceral pain. Note: *compared to the Blank group, $P < 0.05$.

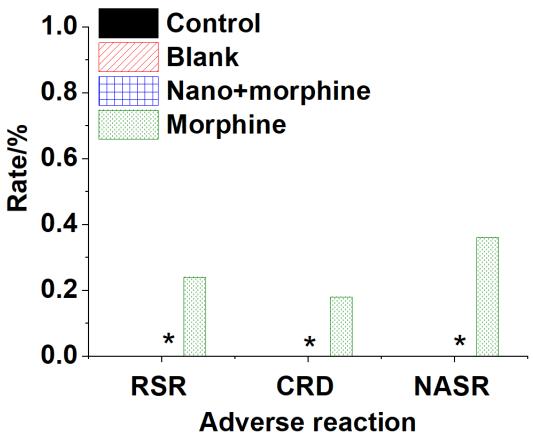

Figure 10. Physiologic toxicity reactions in various groups of mice post-treatment. Note: *compared to the Morphine group, $P < 0.05$.

nists targeting NE and 5-HT receptors, key neurochemical participants in pain perception, were administered, revealing their ability to eliminate conditioned pain modulation associated with pain hypersensitivity [19]. In our study, morphine sulfate nano-controlled release particles reduced levels of NE in the hypothalamus and promoted synthesis and secretion of 5-HT, effectively reducing central nervous system sensitivity to pain. This is consistent with the observed inhibition of pain behavioral responses in mice. Visceral pain in mice often elicits body twisting and localized contractions at the pain site. In this study, morphine sulfate nano-controlled release particles exhibited a significant inhibitory effect on visceral pain response in mice with pancreatic cancer. Research has shown that ART nanocapsules have more effective and longer-lasting analgesic effects compared to free ART or morphine, providing effective pain relief for postoperative pain [20]. Animal studies have also demonstrated that molecularly imprinted chitosan-based nanogels can prolong the time course of morphine-induced analgesia [21], similar to the analgesic outcomes observed with morphine sulfate nano-controlled release particles in this study. Safety testing of this nano-drug in animals in our study revealed that mice receiving morphine sulfate nano-controlled release particles exhibited favorable outcomes with no apparent adverse reactions. In the study by Milanesi et al., the use of thiotic acid-chitosan nanoparticles demonstrated good safety profiles [22]. Numerous studies have highlighted the excellent drug-loading capabilities of chitosan nano-carriers, showing promising results as carriers for oral drugs, cancer drug delivery systems, and more [23, 24]. Chitosan nano-carriers have been clinically used in oral applications without compromising drug efficacy and can extend drug duration [25], indicating broad prospects for chitosan nano-carriers in various applications. The use of morphine sulfate-chitosan nano-controlled release particles in this study holds promise as a new therapeutic agent for visceral pain in future clinical analgesic treatments.

Although this study showed that morphine sulfate nano-controlled release microspheres had good analgesic effects in the short term, there was a lack of data on long-term efficacy and safety, necessitating further research. Additionally, this study only investigated the analgesic effect of morphine sulfate nano-controlled release microspheres in mice. Future studies should involve larger animals to observe the safety and efficacy of high-dose morphine sulfate nano-controlled release microspheres. The tumor pain model established in this study focused solely on the pancreatic cancer pain model, which had certain limitations in the observation effect. Despite these limitations, the results of this study provided strong evidence for the ability of morphine sulfate nano-controlled release microspheres in the treatment of visceral pain caused by tumors. With the advancement of technology and more in-

depth research, this new type of drug delivery system may become a new choice for treating visceral pain in clinical practice. In addition, chitosan nanocarriers have broad application prospects in the field of drug delivery, and this deserves further research.

Conclusion

In this study, the morphine sulfate nano-controlled release microspheres were first prepared and optimized, and their release properties in vitro were investigated. Subsequently, a mouse model of pancreatic cancer tumor pain was established. It was found that morphine sulfate nano-controlled release microspheres exhibited the best drug release performance *in vitro* when the dosage of cross-linking agent was 8:1.

In the treatment of tumor-induced visceral pain, morphine sulfate nano-controlled release microspheres can significantly alleviate visceral pain, inhibit pain behaviors in mice, and exhibit rapid and significant efficacy by increasing the pain threshold, promoting hypothalamic secretion of 5-HT, reducing NE levels, decreasing premonition scores, and prolonging pain relief duration. Importantly, morphine sulfate nano-controlled release microspheres do not lead to increased adverse reactions, demonstrating their excellent safety profile. This study may provide insight for future clinical analgesic treatments for visceral pain.

Acknowledgements

This work was supported by Beijing Municipal Hospital Research and Cultivation Program Project (PX2018017) and Beijing Science and Technology Plan Project (Z2011000055200-87).

Disclosure of conflict of interest

None.

Address correspondence to: Lei Feng, Department of Pain, Beijing Jishuitan Hospital, Capital Medical University, No. 31, Xinjiekou East Street, Beijing 100035, China. Tel: +86-010-58516688; E-mail: Jst_fenglei@sina.com

References

[1] Sousa Correia J, Silva M, Castro C, Miranda L and Agrelo A. The efficacy of the ganglion impar block in perineal and pelvic cancer pain. Support Care Cancer 2019; 27: 4327-4330.

[2] Torres JE, Nagpal AS, Iya A, McGeary D and Srinivasan M. Interventional treatment options for women with pelvic pain. Curr Phys Med Rehabil Rep 2020; 8: 229-239.

[3] Tate JL, Stauss T, Li S, Rotte A and Subbaroyan J. A prospective, multi-center, clinical trial of a 10-kHz spinal cord stimulation system in the treatment of chronic pelvic pain. Pain Pract 2021; 21: 45-53.

[4] Abokhrais IM, Denison FC, Whitaker LHR, Saunders PTK, Doust A, Williams LJ and Horne AW. Correction: a two-arm parallel double-blind randomised controlled pilot trial of the efficacy of Omega-3 polyunsaturated fatty acids for the treatment of women with endometriosis-associated pain (PurFECT1). PLoS One 2020; 15: e0230055.

[5] Wang H, Mo S, Yang L, Wang P, Sun K, Xiong Y, Liu H, Liu X, Wu Z, Ou L, Li X, Peng X, Peng B, He H, Tian Y, Zhang R and Zhu X. Effectiveness associated with different therapies for senile osteoporosis: a network Meta-analysis. J Tradit Chin Med 2020; 40: 17-27.

[6] Mauritz MD, Hasan C, Dreier LA, Schmidt P and Zernikow B. Opioid-induced respiratory depression in pediatric palliative care patients with severe neurological impairment-a scoping literature review and case reports. Children (Basel) 2020; 7: 312.

[7] Liu H and Tang T. Pan-cancer genetic analysis of disulfidptosis-related gene set. Cancer Genet 2023; 278-279: 91-103.

[8] Naoi M, Wu Y, Shamoto-Nagai M and Maruyama W. Mitochondria in neuroprotection by phytochemicals: bioactive polyphenols modulate mitochondrial apoptosis system, function and structure. Int J Mol Sci 2019; 20: 2451.

[9] Koklesova L, Samec M, Liskova A, Zhai K, Büsselberg D, Giordano FA, Kubatka P and Golunitschaja O. Mitochondrial impairments in aetiopathology of multifactorial diseases: common origin but individual outcomes in context of 3P medicine. EPMA J 2021; 12: 27-40.

[10] Chelly JE, Goel SK, Kearns J, Kopac O and Sadhasivam S. Nanotechnology for pain management. J Clin Med 2024; 13: 2611.

[11] Meng Y, Qiu C, Li X, McClements DJ, Sang S, Jiao A and Jin Z. Polysaccharide-based nanodelivery systems for encapsulation, delivery, and pH-responsive release of bioactive ingredients. Crit Rev Food Sci Nutr 2024; 64: 187-201.

[12] Ding C, Bi H, Wang D, Kang M, Tian Z, Zhang Y, Wang H, Zhu T and Ma J. Preparation of chitosan/alginate-ellagic acid sustained-release microspheres and their inhibition of preadipocyte adipogenic differentiation. Curr Pharm Biotechnol 2019; 20: 1213-1222.

[13] Schmauss C and Yaksh TL. In vivo studies on spinal opiate receptor systems mediating antinociception. II. Pharmacological profiles suggesting a differential association of mu, delta and kappa receptors with visceral chemical and cutaneous thermal stimuli in the rat. J Pharmacol Exp Ther 1984; 228: 1-12.
[14] Gentile D, Boselli D, O'Neill G, Yaguda S, Bailey-Dorton C and Eaton TA. Cancer pain relief after healing touch and massage. J Altern Complement Med 2018; 24: 968-973.
[15] Vergo MT, Pinkson BM, Broglio K, Li Z and Tosteson TD. Immediate symptom relief after a first session of massage therapy or reiki in hospitalized patients: a 5-year clinical experience from a rural academic medical center. J Altern Complement Med 2018; 24: 801-808.
[16] Zhang C, Jia R, Dong Y and Zhao L. Preparation and characterization of poly(3-hydroxybutyrate-co-3-hydroxyhexanoate) microspheres for controlled release of buprofezin. Environ Sci Pollut Res Int 2019; 26: 15518-15526.
[17] Liu H, Xiong Y, Zhu X, Gao H, Yin S, Wang J, Chen G, Wang C, Xiang L, Wang P, Fang J, Zhang R and Yang L. Icariin improves osteoporosis, inhibits the expression of PPARγ, C/EBPα, FABP4 mRNA, N1ICD and jagged1 proteins, and increases Notch2 mRNA in ovariectomized rats. Exp Ther Med 2017; 13: 1360-1368.
[18] Wang M, Wu M, Liu X, Shao S, Huang J, Liu B and Liang T. Pyroptosis remodeling tumor microenvironment to enhance pancreatic cancer immunotherapy driven by membrane anchoring photosensitizer. Adv Sci (Weinh) 2022; 9: e2202914.
[19] Nemoto W, Kozak D, Sotocinal SG, Tansley S, Bannister K and Mogil JS. Monoaminergic mediation of hyperalgesic and analgesic descending control of nociception in mice. Pain 2023; 164: 1096-1105.
[20] Elisei LMS, Moraes TR, Malta IH, Charlie-Silva I, Sousa IMO, Veras FP, Foglio MA, Fraceto LF and Galdino G. Antinociception induced by artemisinin nanocapsule in a model of postoperative pain via spinal TLR4 inhibition. Inflammopharmacology 2020; 28: 1537-1551.
[21] Hassanzadeh M, Ghaemy M and Ahmadi S. Extending time profile of morphine-induced analgesia using a chitosan-based molecular imprinted polymer nanogel. Macromol Biosci 2016; 16: 1515-1523.
[22] Milanesi LH, Rossato DR, Oliveira da Rosa JL, D'avila LF, Metz VG, Wolf JF, Reis VB, de Andrade DF, Jank L, Beck RCR, da Silva CB and Burger ME. Topiramate-chitosan nanoparticles prevent morphine reinstatement with no memory impairment: dopaminergic and glutamatergic molecular aspects in rats. Neurochem Int 2021; 150: 105157.
[23] Sachdeva B, Sachdeva P, Negi A, Ghosh S, Han S, Dewanjee S, Jha SK, Bhaskar R, Sinha JK, Paiva-Santos AC, Jha NK and Kesari KK. Chitosan nanoparticles-based cancer drug delivery: application and challenges. Mar Drugs 2023; 21: 211.
[24] Guadarrama-Escobar OR, Serrano-Castañeda P, Anguiano-Almazán E, Vázquez-Durán A, Peña-Juárez MC, Vera-Graziano R, Morales-Florido MI, Rodriguez-Perez B, Rodriguez-Cruz IM, Miranda-Calderón JE and Escobar-Chávez JJ. Chitosan nanoparticles as oral drug carriers. Int J Mol Sci 2023; 24: 4289.
[25] Samiraninezhad N, Rezaee M, Gholami A, Amanati A and Mardani M. A novel chitosan-based doxepin nano-formulation for chemotherapy-induced oral mucositis: a randomized, double-blinded, placebo-controlled clinical trial. Inflammopharmacology 2023; 31: 2411-2420.